HOLISTIC APPROACH AND RECENT ADVANCES IN THE MODELLING OF THE OHAAKI GEOTHERMAL SYSTEM

T.M.P. Ratouis[1], M.J. O'Sullivan[1], J.P. O'Sullivan[1], J.M. McDowell[2], and W.I Mannington[2]

[1]Department of Engineering Science, the University of Auckland, Auckland 1142 New Zealand

[2]Contact Energy, Wairakei Power Station, State Highway 1, Private Bag 2001, Taupo 3352, New Zealand

t.ratouis@auckland.ac.nz julian.mcdowell@contactenergy.co.nz

Keywords: *Ohaaki, Geothermal, Modelling, TOUGH2.*

ABSTRACT

A sequence of three-dimensional numerical models of the Ohaaki geothermal system has been developed at the University of Auckland (UoA) in collaboration with Contact Energy Ltd (CEL) to assist with the sustainable development of the geothermal resource**.** This paper describes the latest computer model of the Ohaaki Geothermal System (called here Model 35446) made up of 35446 blocks and using an irregular numerical grid**.** Model 35446 has a simplified permeability structure based on the geological model provided by CEL which includes nine geological units and discrete vertical structural features (i.e. faults). This paper considers a more holistic approach of reservoir modelling by focusing on the interactions between the different hydrological units and presents the collaborative efforts of UoA and CEL to replicate the overall field behaviour. It was found that permeable faults are paramount for representing some aspects of the behaviour of Ohaaki including the deep pressure recovery recorded in the last few years. The paper also discusses the benefits and limitations of using either a pure water or a water plus carbon dioxide equation of state.

1. INTRODUCTION

The Ohaaki geothermal system lies on the eastern margin of the Taupo Volcanic Zone (TVZ) in central North Island, New Zealand (Figure 1). The Waikato Rivers bisects the Ohaaki system, dividing it into the West Bank and East Banks areas. Drilling started at Ohaaki in 1965 and steam production for electricity generation commenced in 1988 and continues to this date. In the first stage of production, the main bulk of fluid extraction occurred in the East Bank before shifting to the West Bank where higher temperatures and mass flows were encountered (Carey et al., 2013). A sequence of numerical models of the Ohaaki system have been set up by O'Sullivan and co-workers over the years to represent the geothermal system as accurately as possible, understand the key mechanisms at play, and to assist with effective development of the geothermal resource (e.g. Blakeley et al., 1983; Newson and O'Sullivan, 2001; Zarrouk and O'Sullivan, 2006; Clearwater et al., 2011; Clearwater et al., 2014, Ratouis et al., 2017).

As computer hardware and equation-of-state (EOS) modules have improved, numerical models have increased in complexity and evolved into large multi-phase three dimensional models. However, for Ohaaki and other geothermal fields, these improvements come with a large computational run time which can make the calibration process difficult. This is especially true when updating the model, testing various conceptual models, or undergoing uncertainty analysis. With this in mind we developed two models: Model 35446 water + CO_2 and Model 35446 pure water (pw) (Model 35446 refers to both models). The permeability structure of the numerical model was simplified and updated which allowed us to test various conceptual models and recharge theories.

In this paper we are considering a holistic approach in which the geothermal system is approached as a coherent whole whose various units are intimately interconnected and explicable only by reference to the whole. Holistic thinking is based on the idea that the behaviours of the various component parts of a system are best understood in context and in relation to one another and to the whole. In this modelling study instead of matching various data from individual wells, we are interested in the overall behaviour of the system and the effect that the different hydrological units of the geothermal system have on one another.

The pure water model (Model 35446 pw) was developed in conjunction with Model 35446 water + CO_2 model to speed up the calibration of the model. Appropriate scripting tools were developed to allow switching from a pure water model to a two phase CO2-water (EOS2) model and conversely. This paper presents results for Model 35446 (water + CO_2 and pw) as well as a succinct comparison with the previous Model 45250.

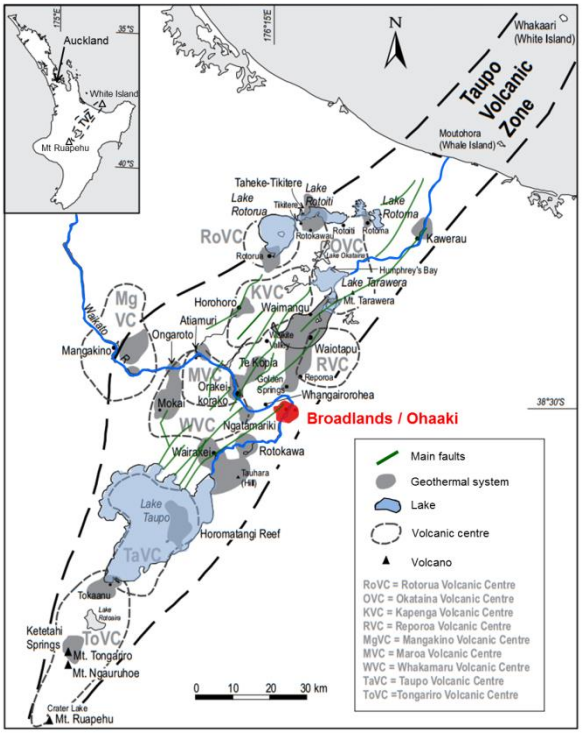

Figure 1: Locations of geothermal fields in the TVZ.

2. OHAAKI GEOTHERMAL POWER PROJECT

Drilling commenced at Ohaaki in 1965, with a total of 44 wells drilled between 1966 and 1984. There was an extended

period of well testing up to 1988, when the Ohaaki Geothermal Power Project (OGPP) was commissioned (Lee and Bacon, 2000; Clotworthy et al., 1995; Carey et al., 2013). The plant commissioned in 1988 had a capacity of 116MWe and during the first 5 years of production, generation was maintained at ~100MWe. In 1993 the available steam began to decline. A deep drilling program was undertaken in 1995 which identified high temperatures and permeability in the deep volcanic formations underlying the West Bank (Lee and Bacon, 2000). A second deep drilling program also focused on the West Bank was undertaken in 2005-2007 (Rae et al., 2007; Carey et al., 2013) allowing generation output to be increased to about 60MWe. Subsequent pressure decline in the deep reservoir led to a reduction in output. Current generation output is maintained at about 45 MWe.

3. OHAAKI GEOTHERMAL SYSTEM

Ohaaki is a high-temperature liquid dominated convective system hosted in the volcaniclastic sequence, sandwiched between the shallow Huka Falls Formation sediments and the greywacke basement (Carey et al., 2013) (Figure 2). Temperatures in excess of 300ºC have been recorded within the greywacke basement (Hedenquist, 1990). The major part of the hot recharge is thought to come through the greywacke via fracture zones from the North-West of the field (Figure 2). The geothermal fluid then flows upwards and eastwards along the greywacke surface. A secondary upflow with higher gas content is believed to come from below the East Bank (Figure 2).

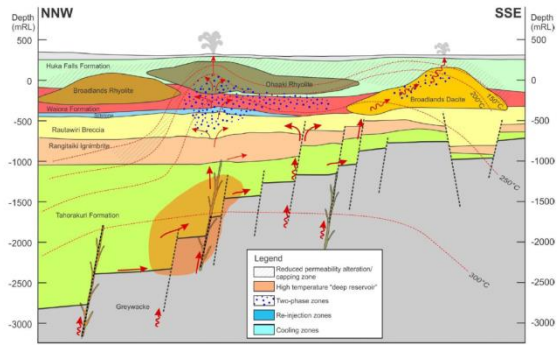

Figure 2: NW-SE cross section of the near natural state conceptual model (Contact Energy Limited, 2015).

In total, five hydrogeological units, located in nine rock groups have been identified at Ohaaki (Figure 4) (Carey et al., 2013) all of which are represented in the numerical model (Table 1):

1. Groundwater: Shallow aquifers from the surface down to approximately an elevation of 200 mRL, generally lying above the Huka Falls Formation.
2. Inner Rhyolite: Hosted in the Ohaaki Rhyolite at depths between 200 and -100 mRL, lying partly over the West Bank production area.
3. Intermediate Aquifer: The original target for production at Ohaaki. A high temperature reservoir at levels between -100 to -900 mRL, generally hosted in the Wairoa Formation.
4. Deep Aquifer: A high enthalpy productive area on the West Bank, below an elevation of about -1200 mRL, hosted in Tahorakuri Formation.
5. Outfield, Outer Rhyolite: Intermediate depth aquifers hosted in cold/cool rhyolite/dacite bodies and hydrologically isolated from the hot productive reservoirs.

Production at Ohaaki has caused pressure decline in the reservoir in response to mass extraction. Fluid will flow (where permeable pathways exist) from high pressure areas to low pressure areas. In the pre-development state these pathways facilitated natural recharge to the system from peripheral areas as well as the natural upflows and outflows from the system such that an equilibrium of inputs and outputs from the system was reached. With extraction and induced pressure change (i.e. away from a natural state equilibrium), these pathways facilitated the movement of variable (including cooler) temperature fluids, thereby altering the thermal regime of the system. Therefore a second conceptual model representing the behaviour of the system during production is required (see Figure 2 and Figure 3). Observations of the productive condition of the field allow the following interpretations:

1. Shallow rhyolites which act as storage for cool fluids and provide conduits for downward migration of fluid to the intermediate reservoir and cause cessation of boiling. This is highlighted by a Temperature decline and pressure recovery in the Intermediate Reservoir post 2000 (Figure 3).
2. A pressure disparity between the intermediate and deep reservoirs suggests a low permeability zone which limits interaction between them. Limited cooling has been observed at depth (Figure 4).
3. The presence of a deep high temperature reservoir which has limited recharge, leading to the onset of boiling when pressure drops sufficiently under production (Figure 3).
4. Pressure recovery in the Deep Reservoir under the West Bank between 2010 and 2015.

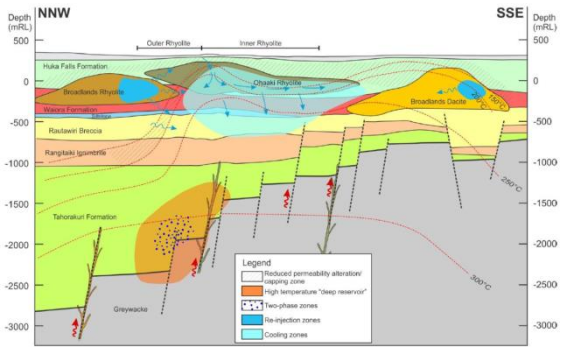

Figure 3: NW-SE cross section of the disturbed conceptual model. (Contact Energy Limited, 2015).

These features enrich the conceptual understanding of the system and provide support for implementing structural and permeability modifications to the numerical model such that natural state and production state observations are captured and are consistently matched with the model. A holistic approach was considered and the present research aimed to match the overall behaviour of the system and to replicate the interactions between the hydrological units listed above.

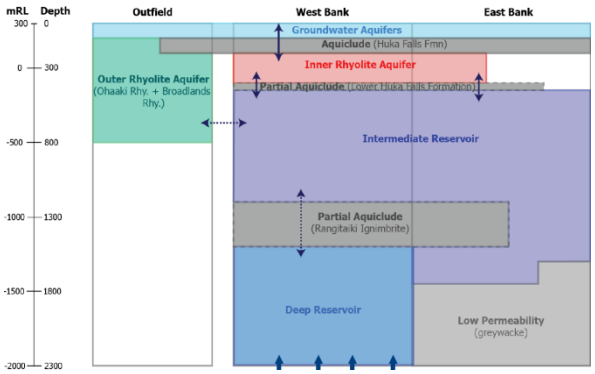

Figure 4: NW-SE cross-sectional illustration of relationship between principal aquifers and aquicludes. Arrows indicate partial leakage allowing some local cross-flows, upflows, or downflows (Contact Energy Limited, 2015).

4. NUMERICAL MODEL OF THE OHAAKI GEOTHERMAL SYSTEM

4.1. Grid structure

Model 35446 is a development of the Ohaaki 45250 model – the layer structure and rotation angle have remained unchanged (Ratouis *et al.*, 2017). Unlike the 45250 grid, the grid for the Model 35446 is irregular with four levels of refinement (Figure 5). Blocks range from 1km by 1km at the outskirts of the model to 250m by 250m in the centre of the model. In the central part of the model, the North-West Bank was further refined, with blocks of 125m by 125m – a quarter of the area of the 250m by 250m blocks used in the Model 45250. Local grid refinement was made in the North West section of the geothermal system to reduce the number of wells located in the same block and to improve the representation of the geological structures while minimizing the computational cost of the simulation.

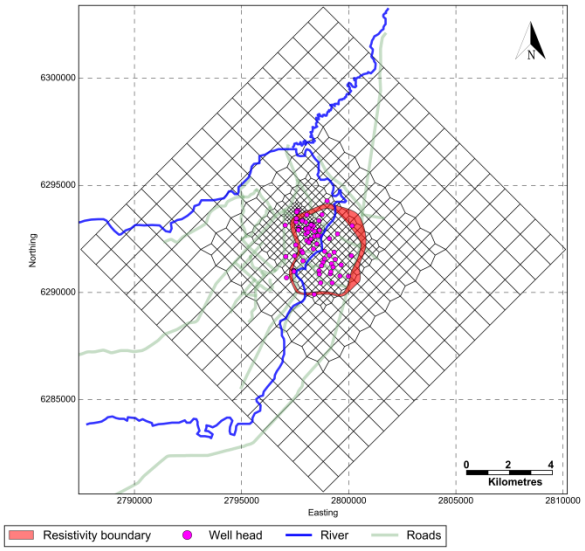

Figure 5: Plan view of the computational grid for the 35446 model. Wellheads are shown in pink.

Figure 5 shows the full extent of the 35446 computational grid and the boundaries of the Ohaaki reservoir. The area covered by the grid extends beyond the resistivity boundary, to ensure all lateral recharge to the Ohaaki geothermal system is captured.

4.2. Geological and Conceptual Model Inputs

4.2.1. A simplified geological structure

The permeability structure of Model 35446 is directly based on the geological model provided by the Geoscience team from CEL. It is made up of 9 geological units identified in the conceptual model of Ohaaki (further divided into 31 rocktypes). Discrete structural features (e.g. faults) were included in the model to reflect our current understanding of the geological structure and the hydrothermal flow of geothermal fluid at Ohaaki. Connection of the shallow and intermediate aquifers was also represented in the model with a high permeability vertical channel in the vicinity of BR9 and the Ngawha geothermal pool. The intention here was to replicate the mechanism for the upflow of deeper fluid to the Ngawha spring as observed in natural state. It was also intended to assist the cooling processes in the production model, once development of the reservoir commenced.

The geological structure of the Ohaaki Geothermal System is represented in the numerical model by rock-type parameters which populate the three-dimensional array of blocks that covers the model area. The rock-type formations are defined to represent the stratigraphy and structure of the geology based on the geological model of Ohaaki. The first two letter of the rock-type assigned in the model represent the geological formation defined in the geological model. There were 670 distinct rocktypes in Model 45250, while Model 35446 has 31 rocktypes, thereby representing a significant reduction in complexity; the properties of the rocktype are directly linked to the geological units defined in the geological model. This allows the numerical model to better study the interactions between the hydrological compartments identified in the conceptual model (Section 3).

Figure 6 shows a NW-SE cross section showing the rock-types used in the numerical model and a NW-SE stratigraphic cross-section through the Ohaaki System.

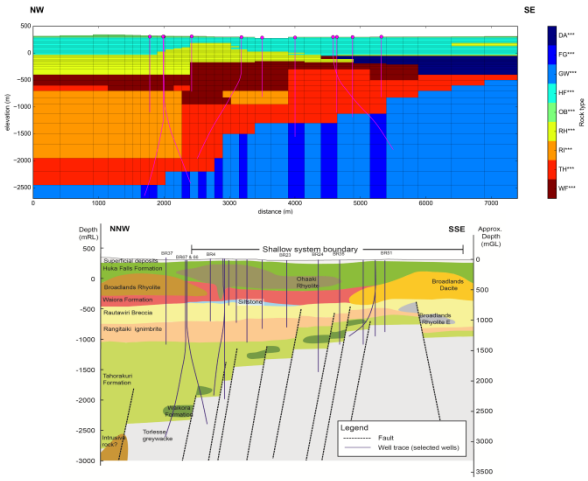

Figure 6: Comparison between the NW-SE cross section showing the rock-types of the 35446 model and the NW-SE cross section of the geological model.

A complete list of the formations used in the numerical model is provided in Table 1.

Table 1: Code and short description of the simplified rock-types groups used in the 35446 Ohaaki model.

Rocktype code	Rock Formation	Hydrological description
OB	Overburden	Shallow groundwater
HF	Huka Falls Formation	Caprock
RH	Rhyolite	Inner rhyolite aquifer
DA	Broadlands Dacite	Outfield intermediate aquifer
WF	Waiora Formation	Original Intermediate Reservoir
RI	Rangitaiki Ignimbrite	Partial aquiclude
TH	Tahorakuri Andesite	Deep Reservoir
GW	greywacke Basement	Low permeability basement
FG	Faulted greywacke	Highly permeable vertical pathways

4.2.2. Implementing a fault network

In the past, due to lack of evidence of structurally controlled permeable pathways and limited by the resolution of the numerical grid, previous models did not include discrete structural features (Newson and O'Sullivan, 2001; Zarrouk and O'Sullivan, 2006; Clearwater *et al.*, 2011; Clearwater *et al.*, 2014). The geothermal upflow from the convective plume at the bottom of the model was averaged over the area of the reservoir. Recent findings and a better understanding of the flow mechanisms suggest that fault structures have a dominant role at Ohaaki by creating pathways for the rising geothermal fluid.

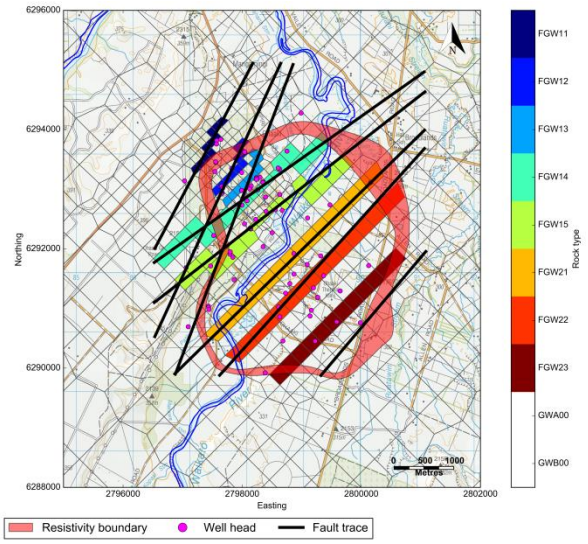

Figure 7: Fault traces from the geological model superimposed on the fault rock-type (FGW) implemented in the Ohaaki numerical grid at -2700 masl.**

The fault network as well as downfaulting of the greywacke basement have been mapped by CEL and GNS Science and included in the geological model. The fault network was implemented in the model by superimposing the geological model on to the numerical model and determining which block each fault passes through (Figure 7). Currently, faults are set vertical and extend to the top of the greywacke basement. The faults are mainly confined to the resistivity boundary where a geothermal upflow is evident. The aim is to achieve a better representation of the geological model in the numerical model.

4.3. Equation of State (EOS)

"Equation-of-state" (EOS) modules govern the thermophysical properties of fluid mixtures needed for assembling the governing mass and energy balance equations (Pruess *et al.*, 1999). They define the number of components and phases in the simulations. For this paper two equations of state were used for Model 35446; a pure water EOS module (EOS1) and water + CO_2 EOS module (EOS2).

EOS1 provides a description of pure water in its liquid, vapour, and two-phase states. All water properties (density, specific enthalpy, viscosity, saturated vapour pressure) are calculated from the steam table equations for pure water as given by the International Formulation Committee (1967) (Pruess *et al.*, 1999). EOS2 is used to describe fluids in gas-rich geothermal reservoirs such as Ohaaki. The presence of CO2 has a large effect on the thermodynamic conditions of a reservoir, especially on temperature distributions and phase compositions (O'Sullivan *et al.*, 1985). The unsaturated zone, between the water table and ground surface is represented by this module and contains water vapour and CO_2.

4.4. Boundary conditions

4.4.1. Base boundary

Heat, mass and CO_2 (for Model 35446 water + CO_2) are injected at constant rates into the bottom of the model to represent natural recharge of the geothermal system.

For areas well outside the reservoir, a background conductive heat flow of 0.120 W/m² is applied. This is a reasonable value for background heat flux for zones close to convective upflows in the TVZ. The heat flux is gradually increased to a maximum value of 0.420 W/m² for blocks close to the main reservoir area representing the greater heat flow anomaly associated with the Ohaaki upflow.

Within the "reservoir area", a deep upflow of high enthalpy water represents the upwelling from the part of the convective plume which has not been captured within the model (i.e. from convective circulation below the base of the model). Recent MT surveys and drilling indicates that the major upflow for the Ohaaki geothermal system is in the North West outside the outer resistivity boundary. In Model 35446 high enthalpy water injected at the bottom of the model is exclusively confined in fault rocktypes (Figure 7); the model has shifted from having an upflow averaged in the West and East Bank to discrete upflows through faults. Deep inflows have been adjusted accordingly and were further calibrated during the natural state calibration process. The CO_2 is injected at an average mass fraction of 1.1%, representative of the amount found in wells at Ohaaki.

4.4.2. Lateral boundary

There are two aspects to determining the horizontal extent of the model. Firstly, the horizontal area of the model is large enough to capture most of the hydrothermal convective

regime at Ohaaki and so that for natural state modelling all side boundaries can be treated as closed.

The second factor to consider with respect to model boundaries is that reservoir behaviour during history simulations should not be subject to boundary effects. Ohaaki has a large boiling zone. The pressure changes in the reservoir are buffered by the expansion and contraction of the boiling zone, and hence do not spread to the edges of the model. Thus, no-flow, closed boundaries are used for all simulations, and checks show that the pressures near the boundaries of the model remain largely unchanged.

4.4.3. Top Boundary

The top surface of Model 35446 water + CO_2 follows the topography of the wider Ohaaki region; topographical data is interpolated with a smooth surface which is used to calculate the top elevation for each column in the model. The top surface is fixed at atmospheric conditions of 15°C, a total pressure of 1 bar, and a partial pressure of CO_2 of 0.9962 bar (giving a partial pressure of water vapour corresponding to 15°C). These "dry" atmosphere blocks sit on top of each column and conditions remain constant throughout the simulation. This allows water vapour and CO_2 to flow freely into the model, and CO_2, water vapour and/or water to flow freely out of the model. The Waikato River and Waiotapu Stream are represented in the model by assigning "wet" atmosphere blocks at the top of columns corresponding to these surface features. Similar to "dry" atmosphere blocks, these allow the setting of a constant pressure and temperature as a top boundary condition. A temperature of 10°C and a hydrostatic pressure corresponding to a water column of 10m was used as the boundary condition. Water can flow freely between the model and these "wet" atmosphere blocks. In addition, an annual average rain fall of 1325mm/yr (Carey et al., 2013) was included at the top of Model 35446. An infiltration rate of 10% has been assumed (Clearwater *et al.*, 2014) and the corresponding amount is injected into all the top blocks in the model, except for those under the Waikato River and Waiotapu Stream.

The top of Model 35446 pw is set at the water table (interpolated from field data) and the temperature and pressure there are fixed at atmospheric conditions – a temperature of 10°C, pressure of 1bar. This acts as a "wet" atmosphere block meaning water can flow in or out of the model. This type of boundary condition is a reasonable approximation if the position of the water table does not vary too much during production and limited shallow boiling occurs.

5. RESULTS OF THE NUMERICAL SIMULATION

5.1. Implementation

The first stage of model development is natural state or steady state modelling. This is aimed at reproducing the conditions of the reservoir pre-exploitation before any production or drilling occurred. The model is run until the reservoir is in a steady state with pressures and temperatures no longer changing. Permeability and deep inflows are adjusted iteratively until the model matches the observed down-hole temperatures of early wells drilled at Ohaaki. This is followed by the production history modelling; the recorded production and injection rates for each well are assigned to the correct block(s) and the model is run for the duration of the production phase. The production history simulation period is from 1966 to 2015. This encompasses early well testing, a recovery period and the operation of the OGPP from 1988 onwards. Calibration of the production history model is made against measured downhole pressure, flowing enthalpy and CO_2 content histories for individual wells. Adjustments to permeabilities and the deep upflows are made as required.

The paper presents a holistic approach to reservoir modelling and will concentrate on the overall behaviour of the field in the various production stages of the OGPP. The model focuses on the interactions between the hydrogeological units at Ohaaki identified in the conceptual model: such as the relationship between the rhyolite aquifers and the Intermediate Reservoir or the hydraulic connectivity between the Intermediate Reservoir and the Deep Reservoir. The model is judged by its ability to reproduce the mechanisms identified in the conceptual model. All results and plots presented below are from Model 35446 water + CO_2 except for the pressure response where results from Models 35446 water + CO_2 and pw are presented. The similarities and differences between the two models are discussed in a separate section. Downhole well temperatures, flowing enthalpy or CO_2 histories for individual wells are not included in the paper. However it was noted that Model 35446 performance is as good as or slightly better than Model 45250 on a well to well basis.

5.2. Intermediate Reservoir

5.2.1. From 1966 to 2001

Figure 8 shows a NW-SE cross section of the modelled **temperature** difference between 2001 and 1966. The model shows an overall temperature decline between the depth of approximately 0 mRL and -900 mRL within the productive area of the field. The temperature drop of 50°C occurs in shallow part of the Intermediate Reservoir. Flow arrows in Figure 8 show a lateral flow and downflow of cold water into the shallow parts of the Intermediate Reservoir. The localised area of temperature increase seen in Figure 8 is caused by the reinjection of the separated geothermal water.

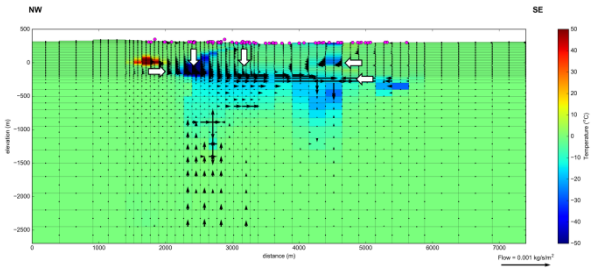

Figure 8: NW-SE cross section showing the model result for the temperature difference between 1966 and 2001. The arrows in white illustrate the recharge mechanisms of the Intermediate Reservoir.

Figure 9 shows the **pressure** difference between 2001 and 1966 in layer 43 (-275 mRL) of the model. The model shows a widespread pressure decline in the Intermediate Reservoir. The East Bank is particularly affected with a pressure drop of approximately 50 bars. Hence the cold water ingress is caused by a large pressure drawdown within the Intermediate reservoir from 1966 to 2001. This allows cold water to flow from the Ohaaki Rhyolite and Outer Rhyolite aquifers into the low pressure areas of the Intermediate Reservoir.

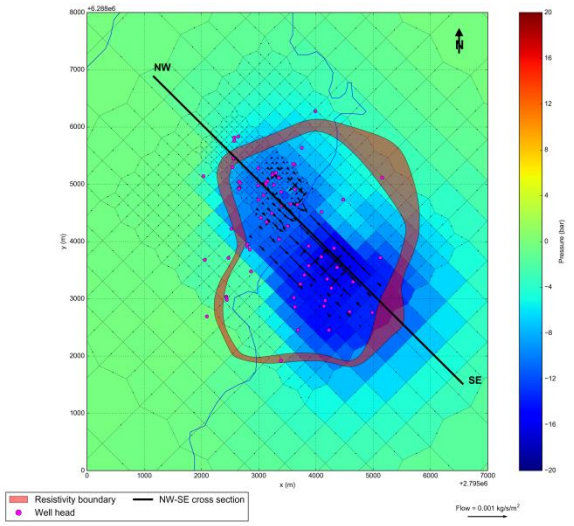

Figure 9: Plan view showing the pressure difference between 1966 and 2001 in layer 43 (-275 mRL) - Intermediate Reservoir - of the Model 35446.

The model replicates only to some extent cessation of boiling within the Intermediate Reservoir identified in the disturbed conceptual model of Ohaaki. Model results shows that **gas saturation** between 1966 and 2001 decreases which indicates a reduction in boiling in the shallow part of the Intermediate Reservoir below the West Bank (Figure 10 and Figure 11). The model shows an increase in boiling below the East Bank (Figure 10 and Figure 11) caused by the decline in pressures and lack of cold water intrusion.

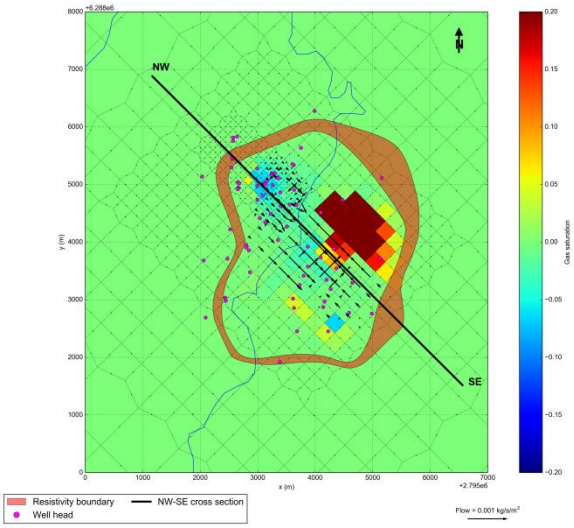

Figure 10: Plan view showing the gas saturation difference between 1966 and 2001 in layer 43 (-275 mRL) - Intermediate Reservoir - of the Model 35446.

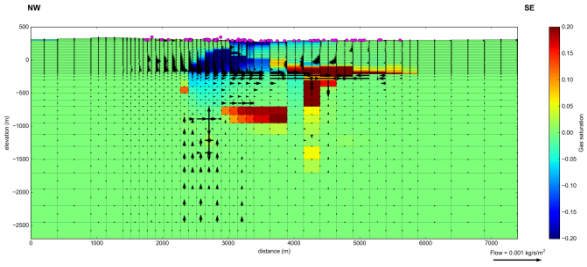

Figure 11: NW-SE cross section showing the gas saturation difference between 1966 and 2001.

5.2.2. From 2001 to 2015

Figure 12 show the **pressure** difference between 2001 and 2015 in layer 43 of the model. The model shows a pressure recovery within the Intermediate Reservoir that is particularly pronounced under the East Bank. This is consistent with the conceptual model and field measurements, as extraction was reduced on the East Bank.

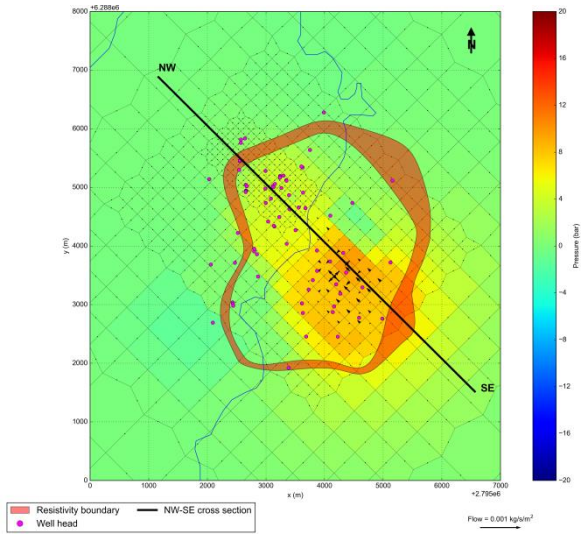

Figure 12: Plan view showing the pressure difference between 2001 and 2015 in layer 43 (-275 mRL) - Intermediate Reservoir - of the Model 35446.

Figure 13 shows the typical pressure transient for a well located in the East Bank within the Intermediate reservoir. The model replicates a 20 bar drop in pressure around 1992 followed by a pressure recovery after 2000. Model 35446 water + CO_2 (blue), Model 35446 pw (black), and Model 45250 (yellow) follow the pressure drawdown very well (Figure 13), however Model 35446 and Model 35446 pw follow the timing and magnitude of the pressure recovery slightly better.

Figure 13Figure 14 shows the results for the pressure response for a well on the West Bank. The trend of the pressure transient in the West Bank is similar to the East Bank. The model replicates a 10 bar drop in pressure around 1992 followed by a pressure recovery after 2000. The results for Model 35446 water + CO_2 (blue) and Model 35446 pw (black) are significantly better than for Model 45250 (yellow) (Figure 14).

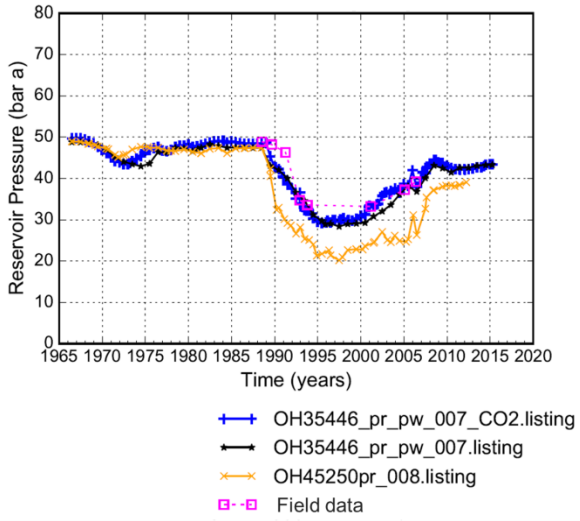

Figure 13: Pressure vs. Time for an East Bank well in the Intermediate Reservoir.

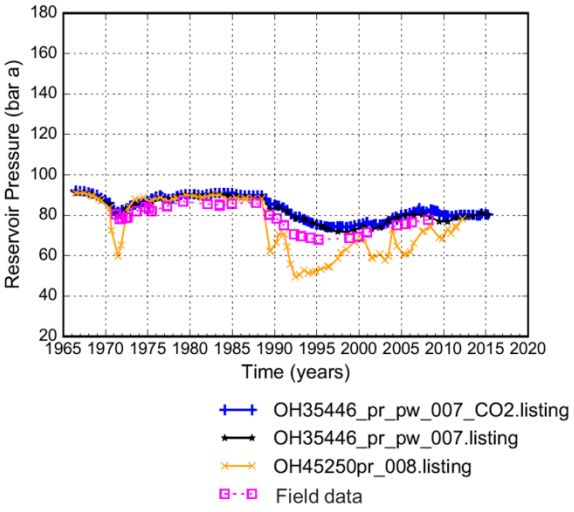

Figure 14: Pressure vs. Time for a West Bank well in the Intermediate Reservoir.

The model is able to replicate the interactions postulated in the conceptual model, e.g., cold water ingress from the rhyolite aquifers into the Intermediate Reservoir caused by a pressure drop. Reduction or cessation of boiling in the Intermediate Reservoir especially in the East Bank is not clear and is an area of current calibration effort.

5.3. Deep Reservoir

Production from the Deep Reservoir started in the years 2000. Figure 15 shows a NW-SE cross section of the modelled **pressure** difference between 2001 and 2010. The model shows a significant decline (approx. 50 bars) in the Deep Reservoir between the depth of approximately -1400 mRL and – 2200 mRL. From 2010 to 2015 the model shows a recovery in deep pressures (Figure 16). Flow arrows in Figure 16 show an upflow of fluid into the Deep Reservoir while a downflow of fluid from the Intermediate Reservoir remains limited. This highlights that, contrary to the behaviour of the Intermediate Reservoir, the pressure decline and recovery in the Deep Reservoir enhances the hot geothermal fluid recharge from below and only a limited amount of colder fluid enters the Deep Reservoir.

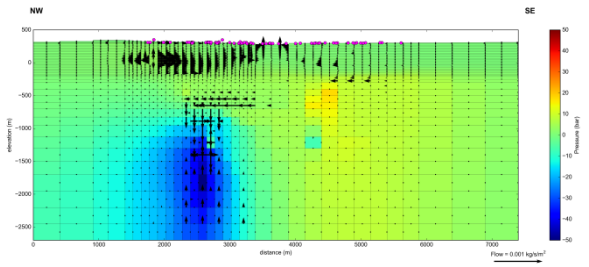

Figure 15: NW-SE cross section showing the pressure difference between 2001 and 2010 of the 35446 model. Well heads are shown in pink.

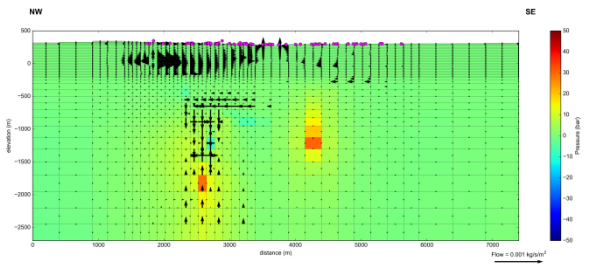

Figure 16: NW-SE cross section showing the pressure difference between 2010 and 2015 of the 35446 model. Well heads are shown in pink.

Figure 17 and Figure 18 show the **temperature** difference during the same period. It shows that the temperature in the Deep Reservoir remains largely stable.

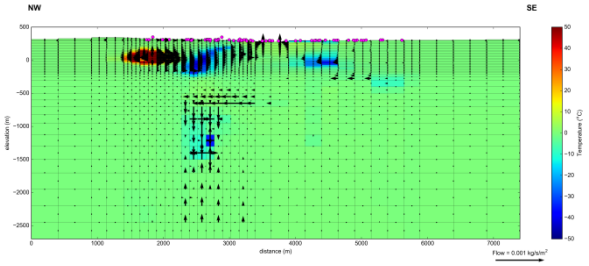

Figure 17: NW-SE cross section showing the temperature difference between 2001 and 2010 of the 35446 model.

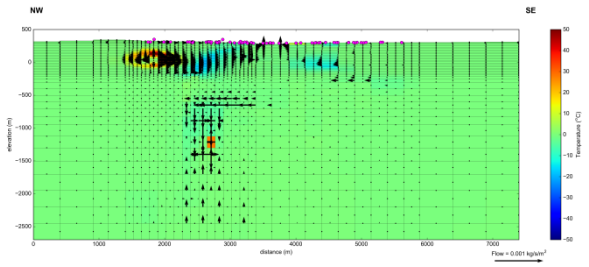

Figure 18: NW-SE cross section showing the temperature difference between 2010 and 2015 of the 35446 model.

Figure 19 and Figure 20 show the pressure response from two wells located within the Deep Reservoir. The match between the results for Model 35446 water + CO_2 (blue) and

Model 35446 pw (black) and the field data is very good and significantly better than for Model 45250 (yellow) where the deep pressure recovery was not replicated Figure 19 and Figure 20.

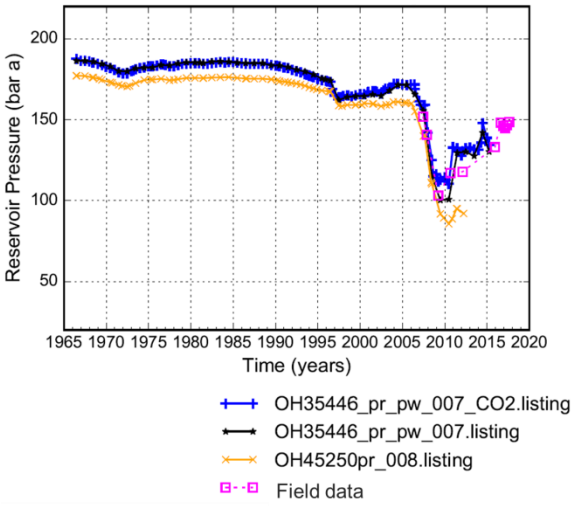

Figure 19: Pressure vs. Time for a West Bank well in the Deep Reservoir.

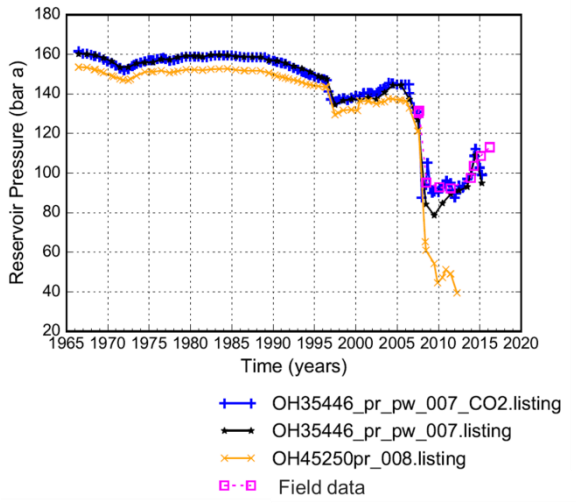

Figure 20: Pressure vs. Time for a West Bank well in the Deep Reservoir.

Model 35446 is able to replicate the very steep and large pressure decline and recovery observed in the Deep Reservoir from 2005 to 2015. One of the key features of models 35446 are the inclusion of faults at the bottom of the model. These represent vertical conduits for the hot geothermal fluid. They appear essential for replicating the pressure recovery recorded in wells located in the Deep Reservoir by allowing deep recharge of the Deep Reservoir.

6. BENEFITS AND LIMITATION OF A PURE WATER MODEL VS WATER PLUS CARBON DIOXIDE MODEL

Model 35446 water + CO_2 and previous Model 45250 both explicitly include the vadose zone which corresponds to the unsaturated zone above the water table. For these models the top of the model is located at the topographical land surface and ambient atmospheric conditions are assumed (with a "dry" atmosphere containing air and water vapour). Thus air and water vapour can move into the model, and water or air and water vapour can flow out (Section 4.4). For this type of model the water table can move freely. These models represent realistically the shallow subsurface and are able to capture the behaviour of surface features, environmental effects such as shallow pressure regime which can be used to better assess shallow water table impacts and subsidence potential. However, a moving water table leads to increased model complexity, a very large computational run-time, and the gas/water models often experience convergence and performance issues (O'Sullivan et al. 2013).

In order to ignore the vadose zone and avoid the complexity of non-isothermal air/water interaction, the water table for Model 35446 pw was set at the top surface of the model. This boundary condition assumes ambient temperature and pressure conditions, with a "wet" atmosphere so water can move in and out of the model. The setting of the top of the model at the water table allows model complexity and the simulation run time to be greatly reduced (Table 2). The computational gain for the pure water model (EOS1) over the water + CO_2 model (EOS2) is equal to 96%. This allowed us to test various models configuration and helped test various recharges set-ups within a reasonable time and proved extremely useful. Figure 13, Figure 14, Figure 19, and Figure 20 and comparison with other data sets (flowing enthalpy, downhole temperature) show that the overall results between Model 35446 and Model 35446 pw are very similar and therefore Model 35446 pw was used for a first stage calibration of Model 35446 water + CO_2. Once a reasonable match was obtained with Model 35446 pw, Model 35446 was modified and run using the water + CO_2 EOS module.

Table 2: Average production run time for Models 45250, 35446 water + CO_2, and 35446 pw

Model	EOS	Production run time
OH45250	EOS2 water+CO_2	10 hours
OH35446	EOS2 water+CO_2	6 hours
OH35446	EOS1 pure water	14 minutes

Python scripts were developed to automate the transition between EOS1 (Model 35446 pw) and EOS2 (Model 35446 water + CO_2). These involve creating a new geometry extending to the topographic surface, populating the new blocks with the appropriate rocktype, modifying surface boundary conditions, and changing the initial conditions for the steady state simulation.

However, it was found that this approach impacted the shallow recharge for the field. In some cases it limited the amount of recharge flowing into production model blocks in the history matching simulations and subsequently introduced convergence issues.

For example, for Model 35446 water + CO_2 and Model 35446 pw, production of geothermal fluid was maintained at 50kg/s in the block highlighted in Figure 21 and Figure 22 (called here block X). In the pure water model the amount of

recharge into the block X is enough to sustain production from this block. In Model 35446 water + CO_2 the amount of fluid flowing into block X is not sufficient to sustain production. Block X in Model 35446 water + CO_2 pressure drops to close to 0 and the block dries out, causing the simulation to stop.

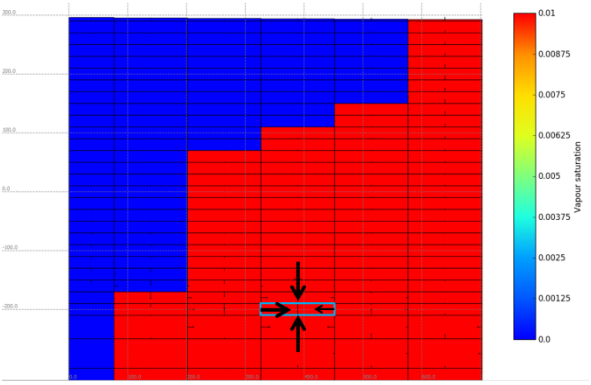

Figure 21: Cross section in the West Bank showing the vapour saturation for Model 35446 pw after 27 years of production.

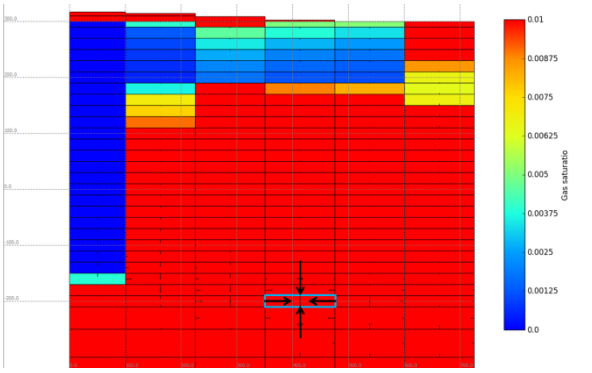

Figure 22: Cross section in the West Bank showing the vapour saturation for Model 35446 water + CO_2 after 27 years of production.

The surface boundary condition in Model 35446 pw allows for an unlimited supply of cold water at the surface. The weight of cold water pushing down allows for vertical downflow supporting recharge in block X. Whereas in the water + CO_2 model the pressure support is not as significant and the water only trickles down which offers less pressure support to block X.

Model 35446 pw cannot therefore be directly used as a substitute for the Model 35446 water + CO_2. In order to sustain production from block X and for the simulation to carry on, the permeability of the rocktype in this area had to be increased to allow more fluid to flow into block X. Therefore using a pure water model may underestimate the permeability as it allows for more pressure support under production than may be realistic. The pure water model is extremely useful as it runs significantly faster but is not a technically correct approximation of reality. In this case, the permeability required to sustain recharge to a production block was underestimated. If Model 35446 pw was used for forecasting purposes it would omit the impact of CO_2 and may incorrectly estimate the level of production the model can sustain.

7. CONCLUSIONS

The paper presents the recent advances in the modelling of the Ohaaki geothermal system. The permeability structure of the numerical model was simplified and updated to match the geological and hydrodynamic models of Ohaaki. The paper also describes a process which uses two different equation of state modules to speed up calibration processes. This made it possible to test a large number of conceptual models, and theories on the deep recharge of the model within a reasonable timeframe.

Secondly the calibration process followed a holistic approach and we focused on the overall behaviour of the field during the different stage of production. By concentrating on the interactions between the various hydrogeological units, we were able to replicate how the condition in the field evolved over time. This in turn facilitated a significant improvement in individual well pressure responses.

This approach helped improve our understanding of the relationship between the deep recharge of the field, the Deep Reservoir and the Intermediate Reservoir. Indications of deep recharge from the NW sector of the field which supports production in the Deep Reservoir is now supported by the numerical model. This was identified as significant gap in earlier modelling and represents a step change in the model calibration quality as well as overall confidence in the model for forecasting purposes. This work has also highlighted areas of the model where improvement is needed such as increasing the hydraulic connectivity between the rhyolite aquifers and Intermediate Reservoir to enhance the intrusion of cold water into the Intermediate Reservoir and cessation of boiling.

ACKNOWLEDGEMENTS

The collaboration on this project between Auckland University and Contact Energy Limited's geothermal department is part of a long standing and fruitful relationship between both parties on the commercial development of the Ohaaki geothermal resource. Both parties are grateful to Contact Energy Limited for permission to publish this paper.

.REFERENCES

Blakeley, M.R., O'Sullivan, M.J. and Bodvarsson, G.S.: A simple model of the Ohaaki Geothermal Reservoir, *Proc. 5th New Zealand Geothermal Workshop*, Auckland, New Zealand, pp. 11-16. (1983).

Contact Energy Limited: *System Management Plan for the Ohaaki Geothermal System*. Ohaaki Geothermal Power Plant. pp. 130. (2015)

Carey, B., Alcaraz, S., Soengkono, S., Mroczek, E., Bixley, P., Rae, A., Lewis, B, Reeves, R. and Bromley, C.: *Ohaaki Geothermal Power Plant. Project Reference Report: Geoscientific and Reservoir Engineering Review*. GNS Science Consultancy Report 2011/273, 236p., (also Appendix C to Part B, the Assessment of Environmental Effects Report, submitted by Contact Energy to the Waikato Regional Council in support of an application for Resource Consents for the Ohaaki Geothermal Power Plant). (2013).

Clearwater, E. K., Brockbank, K., and O'Sullivan, M. J.: An update on modelling the Ohaaki geothermal system.

Proc. 33rd New Zealand Geothermal Workshop. Auckland. New Zealand. (2011).

Clearwater, E. K., O'Sullivan, M. J., Mannington W.I., and Brockbank, K.: Recent Advances In Modelling The Ohaaki Geothermal Field. *Proc. 36th New Zealand Geothermal Workshop*. Auckland. New Zealand. (2014).

Clotworthy, A., Lovelock. B. and Carey, B.: Operational History of the Ohaaki Geothermal Field, New Zealand., Proc. World Geothermal Congress, Florence, Italy, pp. 1797-1802. (1995).

Hedenqvist, J.W.: The thermal and geochemical structure of the Broadlands-Ohaaki geothermal system, New Zealand. Geothermics, 19(2), pp. 151-185. (1990).

Lee, S. and Bacon, L.: Operational History of the Ohaaki Geothermal Field, New Zealand. Proc. World Geothermal Congress, Kyushu-Tohoku, Japan, 2000, pp. 3211-3216. (2000).

Newson, J.A. and M. J. O'Sullivan, M.J.: Modelling the Ohaaki Geothermal System. *Proc. 26th Workshop on Geothermal Reservoir Engineering*, Stanford University, Stanford, California, pp. 186-192. (2001).

O'Sullivan, M.J., Bodvarsson, G.S., Pruess, K., and Blakeley, M.R.: Fluid and Heat Flow in Gas-Rich Geothermal Reservoirs. *Society of Petroleum Engineers Journal, Vol. 25, No. 2, pp.215 – 226.* (1985).

Pruess, K., Oldenburg C., Moridis, G.: TOUGH2 User's Guide, Version 2.0. Lawrence Berkeley National Laboratory Report LBNL-43134, Berkeley, CA. (1999).

Ratouis T., O'Sullivan J.P., and OSullivan M.J. : Ohaaki Reservoir Modelling Report. *Confidential Report. Uniservices and Department of Engineering Science, Auckland. 1-160.* (2017).

Zarrouk, S.J. and O'Sullivan, M.J.: Recent Computer Modelling of the Ohaaki Geothermal System. *Proc. 28th New Zealand Geothermal Workshop*, Auckland, New Zealand. (2006).